

Artificial pseudoneglect:

Connectional constraints leading to the emergence of spatial
bias in neurorobots

Onofrio Gigliotta^{1,2}, Tal Seidel Malkinson³, Orazio Miglino^{1,2}, Paolo
Bartolomeo^{3*}

¹ Department of Humanistic Studies, University of Naples Federico II, Naples, Italy

¹ Institute of Cognitive Sciences and Technologies, National Research Council, Rome, Italy

³ Inserm U 1127, CNRS UMR 7225, Sorbonne Universités, UPMC Univ Paris 06 UMR S
1127, Institut du Cerveau et de la Moelle épinière, ICM, Paris, France

* Corresponding author

E-Mail: paolo.bartolomeo@gmail.com

Short title: Emergence of spatial bias in neurorobots

Abstract

Most people tend to bisect horizontal lines slightly to the left of their true center (pseudoneglect), and start visual search from left-sided items. This physiological leftward spatial bias may depend on hemispheric asymmetries in the organization of attentional networks, but the precise mechanisms are unknown. In this study, we aimed at testing and specifying this hypothesis by modeling relevant aspects of the ventral and dorsal attentional networks (VAN and DAN) of the human brain. First, we demonstrated pseudoneglect in visual search by asking 101 right-handed psychology students to perform a cancellation task. Participants consistently tended to start the task from a left-sided item, thus showing pseudoneglect. Second, we trained five populations of simulated neurorobots to perform a similar task, by using a genetic algorithm. The neurorobots' behavior was controlled by artificial neural networks, which simulated the human VAN and DAN in the two brain hemispheres. The five populations of neurorobots differed in the connectional constraints that were applied to the anatomy and function of the attention networks. Results indicated that (1) neurorobots provided with a biologically plausible hemispheric asymmetry of the VAN-DAN connections displayed the best match with human data, confirming that such connectional asymmetries may well play a causal role in pseudoneglect; however, (2) anatomical asymmetry *per se* was not sufficient to generate pseudoneglect; in addition, the VAN must have an excitatory influence on the ipsilateral DAN for such a bias to consistently occur. These findings provide a proof of concept of the causal link between connectional asymmetries and pseudoneglect, and specify important biological constraints that result in physiological asymmetries of human behavior.

Author summary

When exploring our environment, most of us tend to start their exploration from the left side. In this study, we first provided a demonstration of this tendency in a population of undergraduate students, who tended to start a visual search task by detecting a target on the left side of the display. We then investigated the possible mechanisms of this spatial bias by training artificial agents (neurorobots) to perform a similar visual search task. The neurorobots' behavior was controlled by artificial neural networks, whose architecture was inspired by the human fronto-parietal attentional system. In five distinct populations of neurorobots, different constraints were applied on the connections of the attentional networks, within and between the brain hemispheres. Only one of the artificial populations demonstrated a spatial bias that closely mirrored that shown by the human participants. The specific connectional constraints applied to this population included known characteristics of the human fronto-parietal networks, but had also additional properties not previously described. Thus, our findings specify important biological constraints that result in physiological asymmetries of human behavior.

Keywords: Spatial exploration, Visual search, Attention, Brain connections,
Spatial neglect

1. Introduction

A thorough exploration of the space around us is essential to everyday life. However, spatial exploration is not perfectly symmetrical in humans. For example, when marking the center of a horizontal line, most of us deviate slightly to the left of its geometric center [1, 2]. Bowers and Heilman [1] termed “pseudoneglect” the physiological leftward bisection error, because it occurs in the direction opposite to the rightward shifts typical of patients with right hemisphere damage and signs of visual neglect [3]. In a similar way, when we explore a horizontal A4 sheet in order to cancel out visual targets, we tend to start the search from the left part of the sheet [4, 5]. In addition, leftward spatial bias can occur in such diverse contexts as tactile rod bisection [6], picture scanning [7, 8], simulated driving [9], spatial navigation [10] (but see [11]), rapid serial visual presentation [12], processing of facial emotions [13], and even mental imagery [14, 15]. In these cases, exploratory behavior typically starts from the left side more often than it does from the right side or from the center. As a consequence, the term “pseudoneglect” has also been applied to these forms of leftward spatial bias, by analogy to pseudoneglect on line bisection. Interestingly, right hemisphere damage can reverse this lateral bias. As a matter of fact, a reversed bias with a right starting side constitutes the most sensitive index of spatial bias in patients with right hemisphere damage, even in the absence of signs of left neglect [4, 16, 17].

Evidence shows that visuospatial attention is a major determinant of pseudoneglect [18, 19], although cultural factors such as reading habits may also contribute [20]. It has thus been suggested that pseudoneglect mainly results from asymmetries in the hemispheric control of attention [7, 21]. However, the specific neural structures and the mechanisms at the basis of pseudoneglect remain unknown.

In the human brain, visuospatial attention is controlled by fronto-parietal networks, which demonstrate substantial asymmetries across the hemispheres

[22, 23]. We now know several details on the anatomical organization [24] and functional characteristics [25] of these networks, and how their dysfunction in the right hemisphere can lead to signs of neglect for left-sided events [26, 27]. When normal participants perform cued detection tasks [28], a bilateral dorsal attentional network (DAN), composed by the intraparietal sulcus / superior parietal lobule and the frontal eye field / dorsolateral prefrontal cortex, shows increased blood oxygenation level dependent (BOLD) responses during the cue – target period [25]. Thus, the DANs appear to be important for spatial orienting towards contralateral events. The same studies also demonstrated the presence of a ventral attentional network (VAN), which includes the temporoparietal junction and the ventral frontal cortex (inferior and middle frontal gyri), and shows increased BOLD responses when participants have to respond to invalidly cued targets [25]. Thus, the VAN is considered important for detecting unexpected but behaviorally relevant events, by inducing the DANs to reorient attention towards these events. Importantly, the VAN is strongly lateralized to the right hemisphere, whereas the DAN is bilateral and symmetric (although other studies have provided some evidence of right lateralization of the DAN [29-31]). The DANs are also crucial for abilities interacting with attention, such as visual working memory [32]. Anatomically, three branches of a long-range white matter pathway, the Superior Longitudinal Fasciculus (SLF), connect these networks. Evidence obtained with advanced white matter tractography [24] demonstrated that the SLF has a ventro-dorsal gradient of hemispheric asymmetry. The ventral branch of the SLF connects the VAN and is anatomically larger in the right hemisphere than in the left hemisphere, whereas the dorsal branch (connecting the DAN) is more symmetrical. The lateralization of the intermediate branch of the SLF displays interindividual differences, and is strongly correlated to the individual amount of spatial bias in line bisection and in the speed of detection between the right and

the left hemifield. Specifically, larger SLF volumes in the right hemisphere correlate with larger leftward bias [24].

A further potential source of performance asymmetry resides in the pattern of inter-hemispheric connections. Behavioral and electrophysiological evidence suggests that inter-hemispheric communication is not strictly symmetrical in humans, but it is faster from the right to the left hemisphere [33]. Also, the posterior callosal connections from the right parietal node of the DAN to its left hemisphere homologue seem to be predominantly inhibitory [34]. Concerning the VAN, its right and left temporo-parietal caudal nodes are not strongly connected by callosal fibers [35], and thus work in relative isolation from one another.

It is tempting to relate these biological constraints to the widespread leftward bias that occurs in human exploratory behavior. However, little is known about the specific dynamic interplay between the attentional networks resulting in spatial bias. On the one hand, methods used in humans have substantial limitations of spatiotemporal resolution and of inferential power, which severely limit their scope. On the other hand, it is difficult to draw firm conclusions from monkey neurophysiology, because of important differences between humans and primates in the organization of attention networks [36]. In the present study, we took a different approach to unravel these issues. First, we tested a group of human participants to establish the presence and characteristics of pseudoneglect in a visual search task (Experiment 1). In Experiment 2, we trained neurally controlled robots (neurorobots) to perform a task as similar as possible to the human one. We then articulated detailed implementations of several instances of attention network architecture, which directed the neurorobots' performance, in order to identify the structural and functional network constraints crucial for simulating human performance.

2. Experiment 1: Pseudoneglect in human visual search

2.1 Introduction

Pseudoneglect has been mainly measured using tasks of perceptual estimation of the length of horizontal lines [2, 19]. Analogous leftward biases seem also to occur in visual search tasks, as a tendency to find first targets on the left side of the display [4, 37], but evidence in this domain is less systematic. Thus, in the present context it was important to test our specific task in order to ensure the validity of the human-robotic comparison of performance.

2.2. Methods

2.2.1. Ethics Statement

The procedure was approved by the Department of Humanistic Studies of the University Federico II of Naples.

2.2.2. Participants

A total of 101 right-handed psychology students (76 females; mean age \pm SD, 22.24 \pm 4.40) gave their informed consent to perform a visual search experiment for course credit. Participants were recruited in November 2016.

2.2.3. Procedure

The task was designed to be as close as possible to that performed by neurorobots (see section 3 below). Participants were instructed to cancel as fast as possible targets displayed on a touch-sensitive tablet (Mediacom Winpad 801 8-inches, 120 dpi, 1280x800 pixels, refresh frequency 60 Hz), by using a stylus pen. Participants were comfortably seated with a viewing distance of ~40 cm. Each session consisted of 30 trials. Each trial was initiated by the participant touching a green round button placed at the center of the screen. Subsequently, a set of 5

dark-red (HEX #800000) filled round targets, with a 40-pixel radius (0.76° visual angle), was presented. Targets were randomly scattered on a display area of 512x512 pixels ($9.7^\circ \times 9.7^\circ$), placed at the center of the screen. Upon participant's touch, cancelled targets became bright red (HEX #FF0000). To assess lateral bias, we first defined the center of the display as 0, so that the values of the X coordinate went from -256 pixels (-4.85°) on the extreme left to +256 pixels ($+4.85^\circ$) on the extreme right. Second, we measured the average position on the X axis of the first cancelled stimulus for each trial.

2.3. Results

As expected with this easy task, accuracy was at ceiling, with all participants correctly cancelling all the targets. Results showed a left-biased distribution of the first found target (see Fig. 9A below). The average X value was -80.23 pixels (-1.52°), which significantly differs from the central position at $X = 0$ (Wilcoxon-Mann-Whitney two-tailed test, $Z=-6.37$, $p<0.001$).

2.4. Discussion

During a visual search task similar to that used for our simulations, normal participants exhibited a leftward bias (pseudoneglect), consisting in a significant tendency to start the visual search from a left-sided target. This result was observed in an experimental setting as close as possible to that used for neurorobots, and replicates and extends previous results obtained with different types of visual search tasks, such as the line cancellation test [4] and the bells test [37].

3. Experiment 2: Visual Search in Neurorobots

3.1. Introduction

A neurorobot is a real or simulated robot whose behavior is controlled by an artificial neural network. For the present experiment, we developed distinct populations of simulated neurorobots controlled by artificial neural networks with different connectivity constraints.

3.2. Models

The simulated robot (Fig. 1) has a single artificial eye and an actuator (simulated hand) able to perform the cancellation task. The robot's eye can move and zoom, and can thus be described as a pan/tilt/zoom camera, because it can move along the horizontal and vertical axes and can zoom in a range between 1x to 12x. The use of a zoom was inspired by models of attention, which stipulate that attention can either be distributed over the whole field, but with low resolving power, or be continuously constricted to small portions of the visual field with a concomitant increase in processing power [38].

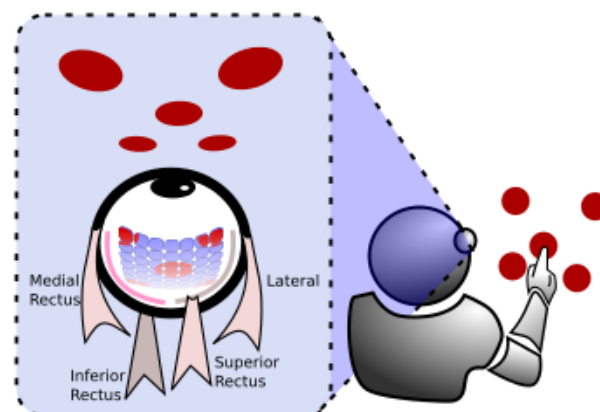


Figure 1. Schema of the neurorobot equipped with an artificial eye, provided with a 7x7 light receptor retina, and controlled by two couples of simulated extraocular muscles.

The artificial eye is equipped with a retina made up of a 7x7 grid of light receptors (see Fig.1). Each receptor outputs an activation value computed by averaging the luminance of the perceived stimuli across the receptive field, with radius set to 80 pixels. Receptors are evenly distributed within the artificial retina, which has a square form with a side varying from 1120 pixels (no zoom) to 96 pixels (maximum zoom). Thus, each stimulus can occupy a retinal surface ranging from 0.8% to 100% of the artificial retina. Horizontal and vertical movements of the eye are controlled by four simulated muscles [39] (see Fig. 1), in analogy to the medial, lateral, inferior and superior recti of the human eye.

3.2.1. Neural network

We used a standard neural network model in which each node of the network has a sigmoid activation function $\varphi(x)=1/(1+e^{-x})$ and an adjustable threshold ϑ . The output, O , is computed for each node i by using the following equation:

$$O_i = \varphi(A_i)$$

Where:

$$A_i = \vartheta_i + \sum_{i,j} w_{ij} O_j$$

w_{ij} is the synaptic weight connecting unit j with unit i . The pattern of connections between nodes has been chosen according to biological evidence on dorsal and ventral attentional networks in human brains (see below, section 3.5).

Fig. 2A depicts the general template network. The 7x7 retina, consisting of 49 artificial neurons, constituted the input layer. The output layer controlled the zoom with two artificial neurons, the extraocular muscles with four neurons, and a decision unit for target detection, which triggered the touch response when exceeding a criterion threshold of 0.7. The hidden layer contained the attention networks and a hidden network devoted to control vertical eye movements (4

neurons, not depicted in Fig. 1). We modeled the DAN and the VAN by building a neural model organized across two hemispheres, with visual information from each visual field projecting to the contralateral hemisphere. Each DAN had 5 artificial neurons; each VAN had 4 artificial neurons. The VAN-DAN connections in the right hemisphere outnumbered those in the left hemisphere, in order to simulate analogous results for the human SLF II [24].

The inter-hemispheric connections were also modeled by following anatomical and functional results obtained in the human brain, and outlined in the Introduction. Thus, (1) they connected only the DANs, but not the VANs, which thus worked in relative isolation from one another (see Fig. 9.4D in Ref. [35]) and (2) they were inhibitory, such that each DAN inhibited the contralateral one [see 34]: each DAN induced contralaterally-directed eye movements and inhibited ipsilaterally-directed eye movements. The DANs controlled zooming and cancellation behaviors. All the hidden units within the DANs also had reentrant connections, which integrate the previous input with the current one, thus simulating a sort of simplified visual memory, in analogy to similar mechanisms occurring in the primate brain [32]. Thus, reentrant connections resulted in some persistence of the previous inputs across steps within a given trial. The model also included an efference copy of movements, sent from the output layer to the input layer within each hemisphere.

3.2.2. Cancellation task

Similar to the human experiment (see section 2), neurorobots performed a 30-trial cancellation task. Targets were presented on a virtual display measuring 512 x 512 pixels. At the start of each trial, the gaze of the artificial eye was initialized at the center of the display, with no zoom. Again, similarly to the human experiment, each trial consisted of a set of 5 round targets, with a luminance value of 0.5 (in conventional units ranging from 0 to 1.0) and a radius of 40 pixels, randomly

scattered in the virtual display. Upon cancellation, targets increased their luminance to the maximum value of 1.0.

3.2.3. The Adaptive/Learning process

For the present work, neurorobots were trained by means of a Genetic Algorithm, a form of evolutionary computation that implements a Darwinian process of adaptation that can model cognitive development and trial-and-error learning, especially when only distal rewards are available [40, 41]. A typical experiment starts with the generation of a random set of individual neurorobots (each defined by a specific set of parameters of a neurocontroller). Each individual is then evaluated according to a fitness function representing the desired performance on a requested task. Due to genetic operators such as mutation and crossover, the best individuals will populate the next generation. The process iterates until a specific performance or a fixed number of generations is reached. In the present work, each genetic string encodes the value of synaptic connections w_{ij} and neuron thresholds in the range (-5, 5). Initially, for each evolutionary experiment a set of 100 random individuals (i.e., competing sets of parameters for the neural network of the neurorobot) were generated and evaluated for their ability to find targets. Targets had to be found as fast as possible on each of 30 cancellation trials, lasting 700 time steps each. At the end of the evaluation phase, individuals were ranked according to their performance, and the best 20 were used to populate the next generation after having undergone a mutation process. Each parameter was encoded by an 8-bit string, thus mutations were implemented by bits switching with probability $p=0.01$. The number of generations was set to 3,000.

Three behavioral components contributed to the overall fitness, F : an exploration component, a component proportional to the number of target correctly cancelled, and a reward for responses promptness.

The exploration component, which was introduced to avoid the bootstrap problem [40], rewarded the ability of the neurorobot to explore its visual field. In particular, the area that can be explored through eye movements was split in 100 cells. Exploration fitness (EF) was then computed for each trial by dividing the number of visited cells by 100. A second fitness component (TF) was represented for each trial by the number of correctly cancelled targets divided by 5 (i.e., the total number of presented targets). Finally, a reward for promptness (PF) was given when all the five targets were cancelled. PF was inversely proportional to the number of time steps nt , used to cancel all the stimuli:

$$PF=nt/700$$

The overall fitness was calculated as

$$F=EF+TF+PF.$$

After training, neurorobots' performance in the cancellation task was evaluated on 30 new trials, in order to measure their accuracy in finding the targets and the position of the first cancelled target, as estimated by the average value of the X coordinate of the first cancelled stimulus across trials.

3.2.4. Valence of VAN-DAN connections

A set of 5 populations of neurorobots, each composed of 40 individuals, featured neurocontrollers with different connectional constraints.

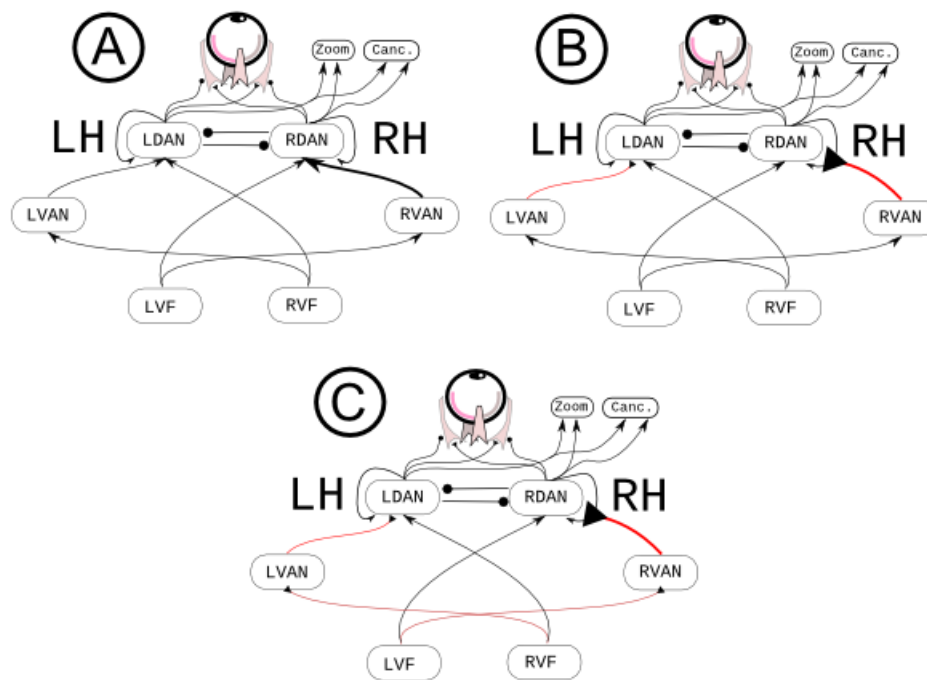


Figure 2. Neurocontrollers A, B and C. Arrows indicate connections that can be either excitatory or inhibitory; red connections with triangular arrowheads denote excitatory connections; round arrowheads represent inhibitory connections. LH, left hemisphere; RH, right hemisphere; Canc., cancellation units: LDAN and RDAN, dorsal attention networks in the left and in the right hemisphere, respectively; LVAN and RVAN, ventral attention networks in the left and in the right hemisphere; LVF and RVF, left and right visual field. Right and left VANs have the same number of neurons, but different patterns of connection strength.

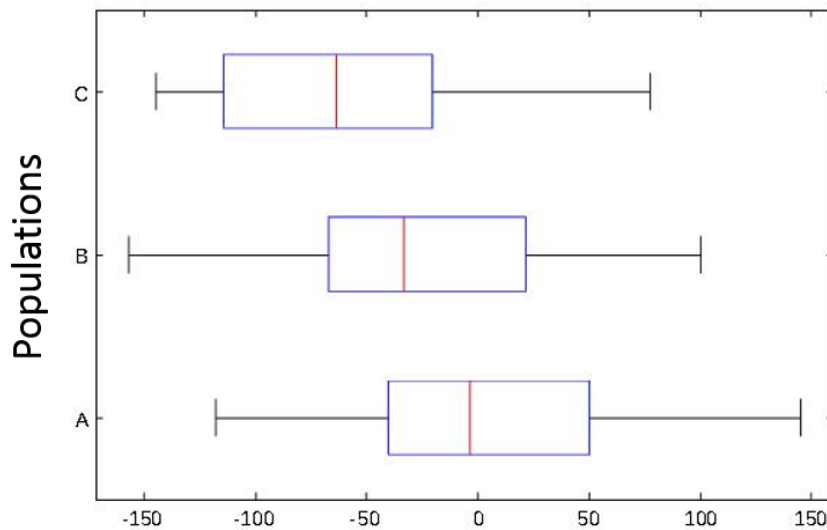
Neurocontrollers A, B and C (Fig. 2) had left-right asymmetric connections between VAN and DAN (i.e., the simulated SLF II), with a greater number of connections in the right hemisphere (120) than in the left hemisphere (108). The ratio of this asymmetry difference (0.05) corresponds to the average asymmetry ratio of SLF II in 20 human subjects, as described by Thiebaut de Schotten et al. [24] (see their supplementary Table 1). In neurocontroller A (Fig. 2A) there were no

constraints in terms of type of connections (inhibitory or excitatory) along the ventral and dorsal attentional networks. In neurocontroller B a further constraint was added: VAN to DAN pathways were set to be excitatory during the training process (see Fig. 2B). Finally, in neurocontroller C also the connections projecting from the retina to the VAN were set to be excitatory (see Fig. 2C). To better evaluate the effect on performance of SLF II asymmetry, we trained two additional control populations based on neurocontroller C: C_0 with completely symmetrical VAN-DAN connections (laterality ratio = 0); C_1 with VAN-DAN connections only present in the right hemisphere, and absent VAN-DAN connections in the left hemisphere (complete right lateralization of SLF II).

3.3. Results

3.3.1. Behavioral Results

Figure 3 reports the performance of the three populations equipped with neurocontrollers A, B, and C on correct cancellations. Each boxplot contains data collected for 40 neurorobots tested on 30 cancellation tasks.



Average abscissa of the first cancelled targets [pxl]

Figure 3. Average x values of the first cancelled target, computed across 30 trials for each population of 40 neurorobots provided with neurocontrollers A, B, and C. The middle bar of the boxplot indicates the median of the tested population. The left side and the right side of the box indicate respectively the first (q1) and the third (q3) quartiles. Whisker length extends until the last data point that is not considered as an outlier, i.e. a point that is greater than $q3 + 1.5 \times (q3 - q1)$ or less than $q1 - 1.5 \times (q3 - q1)$. There were no outliers in the current dataset.

There were no significant differences in the percentage of correct cancellations across the three populations [Kruskal-Wallis test, $\chi^2_{(2, n = 120)} = 1.44, p = .49$]. However, the position of the first cancelled target (X value for each trial) did differ across the tested populations, $\chi^2_{(2, n = 120)} = 18.41, p < .001$. While the position of the first cancelled target was not different from 0 (central position) in neurorobots equipped with neurocontroller A (Wilcoxon-Mann-Whitney, $p=0.1$, two-tailed), the remaining neurorobots tended to start their exploration of the display on the left of the center (neurocontroller B, $Md = -33.27, z = -2.057, p = 0.02$; neurocontroller C, $Md = 63.29, z = -5.35, p < .001$), thus showing a leftward bias reminiscent of human pseudoneglect. The control populations with complete SLF II symmetry

(C₀), or extreme rightward SLF II asymmetry (C₁) showed the predicted patterns of performance: no pseudoneglect for C₀ (Md=20.435, z=-0.823, p=0.411), and large pseudoneglect for C₁ (Md=-96.526, z=-7.406, p=1.299*10⁻¹³) (Fig. 4).

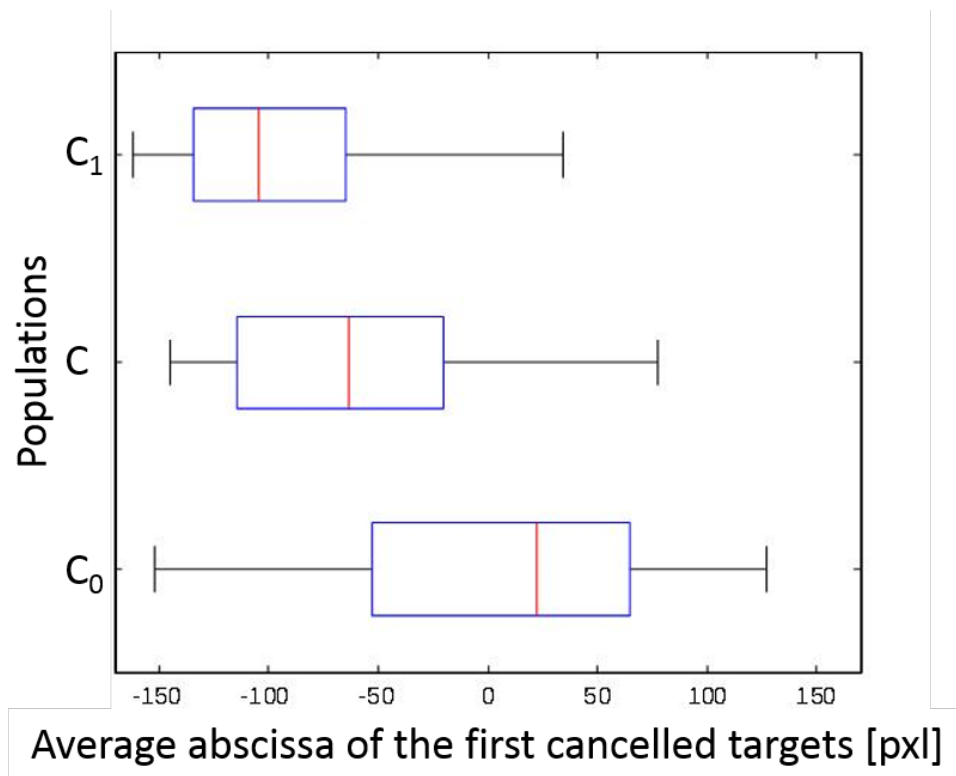


Figure 4. Average x values of the first cancelled targets, for all the neurorobots provided with neurocontrollers C₀, C, and C₁. Average x values of neurorobots C₀ is not significantly different from 0, while average x values of neurocontrollers C and C₁ significantly differ from 0.

3.3.2. Neural results

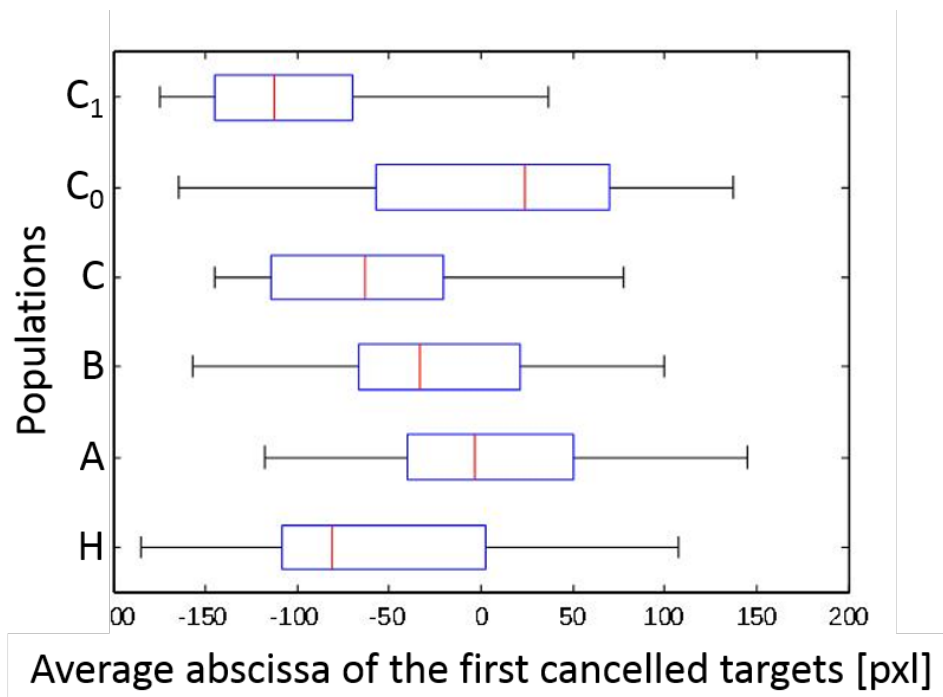


Figure 5. Average position on the X axis of the first cancelled targets for human participants (H) and artificial neurorobots equipped with neural networks A, B, C, C₀ and C₁.

To better understand the neural dynamics leading to the exploratory bias, we examined the average activations of the DANs across all the individuals for each population, equipped with neurocontrollers C (biologically-inspired asymmetry) and C₀ (symmetrical attention networks). We then computed a laterality index of DAN average activations between the two hemispheres: $(\text{Mean Right DAN activation} - \text{Mean Left DAN activation}) / (\text{Mean Right DAN activation} + \text{Mean Left DAN activation})$, with a possible range from -1 (prevalent left DAN activity) to +1 (prevalent right DAN activity). Figure 6 reports the course of the laterality index across time steps. As expected, left and right DAN activations were balanced with neurocontroller C₀. On the other hand, in neurocontroller C activations were unbalanced toward the right hemisphere DAN. A crucial aspect for pseudoneglect

concerns the initial time steps in which the exploratory bias occurs. A higher imbalance toward the right hemisphere DAN is present at the outset of the cancellation task for neurorobots C, as a consequence of asymmetries in their network architecture, while it is obviously absent for neurorobots C₀, with symmetrical networks. The initial imbalance favoring the right hemisphere DAN is the likely basis of the spatial bias towards the initial cancellation of a left-sided item in neurorobots C.

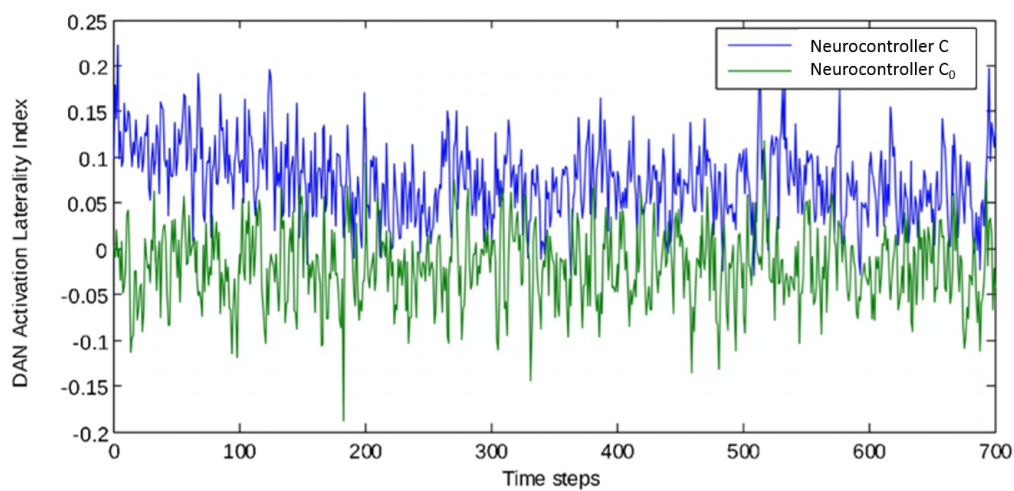


Figure 6. Laterality indexes of DAN activation computed for individuals equipped with neurocontroller C and C₀. A value of 0 means that activation in left and right hemisphere DANs is balanced; positive values denote prevalence of right hemisphere DAN, negative values indicate prevalence of left hemisphere DAN.

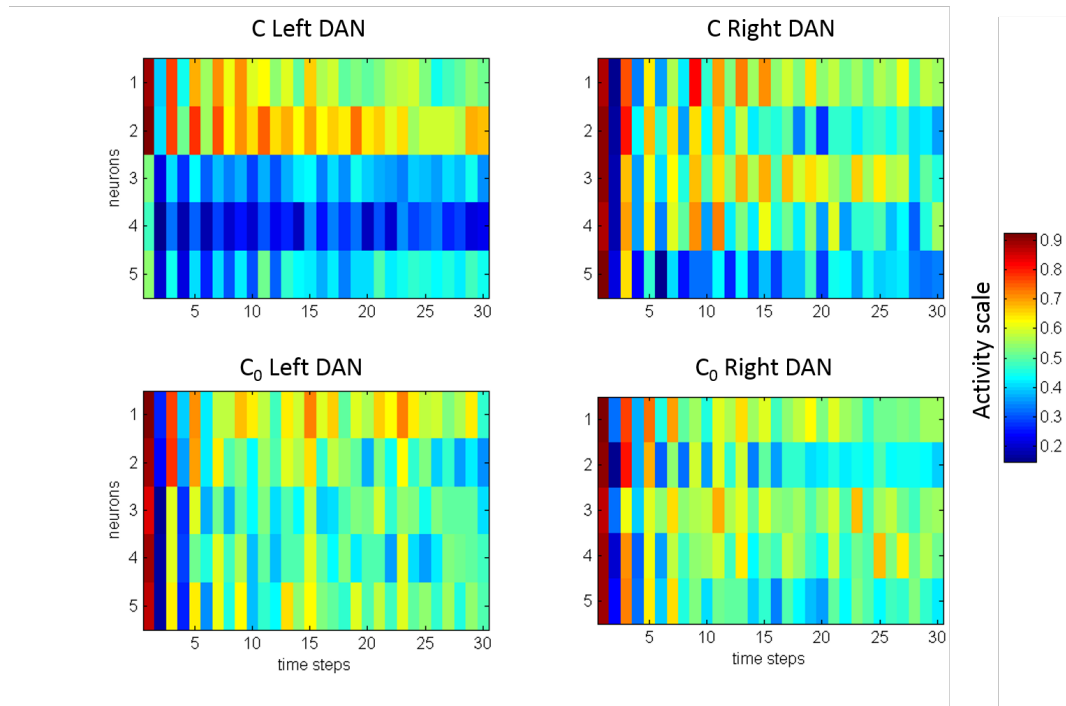


Figure 7. Average activation of hidden neurons in right hemisphere DAN and in left hemisphere DAN, for the first 30 steps of individuals equipped with neurocontrollers C and C_0 . The activity scale goes from 0 (blue) to 1 (magenta). Note the early, large left-right asymmetry in neurobiologically inspired C agents (arrows), which subsequently decreases. The symmetrical C_0 agents do not show any asymmetry of performance.

Figure 7 shows the average activation of the hidden DAN neurons in the left and in the right hemisphere during the first 30 time steps of the cancellation task, for agents equipped with the biologically inspired neurocontroller C, and for those equipped with the symmetrical neurocontroller C_0 . The initial activation is symmetrical for the C_0 agents, but it is higher in the right hemisphere than in the left hemisphere for the C agents. Thus, an asymmetry of VAN connections results in a corresponding activation asymmetry in the anatomically symmetrical DANs. The DAN asymmetry in the initial phases of the task is the simulated neural correlate of behavioral pseudoneglect. After the initial phase, the left-right differences are absorbed by the increased activity of the hidden units; when left and right activities reach saturation, the behavioral asymmetry decreases (see Fig.

6, where asymmetry of performance decreases around time step 150 for neurocontroller C).

3.3.3. Comparison between human and robotic performance

Human participants and robotic populations as a whole did not show the same distribution of the position of the first cancelled targets (Kruskal-Wallis test, $\chi^2(5, n = 301) = 67.88, p < .001$). Post-hoc tests (Dunn's test with Bonferroni correction) demonstrated a difference in distribution between humans and neurocontrollers A ($p < .001$), B ($p=0.0394$), C_0 ($p < .001$), C_1 ($p = 0.0153$). However, the position distribution derived from human performance and neurocontroller C's performance showed a similar degree of leftward asymmetry (Fig. 8; Dunn's test, $p = 1.0$; Levene test of homogeneity, $p = 0.39$). Thus, all robotics agents performed differently from humans, except from the neurocontroller C neurorobot population, whose performance provided a good approximation to human performance.

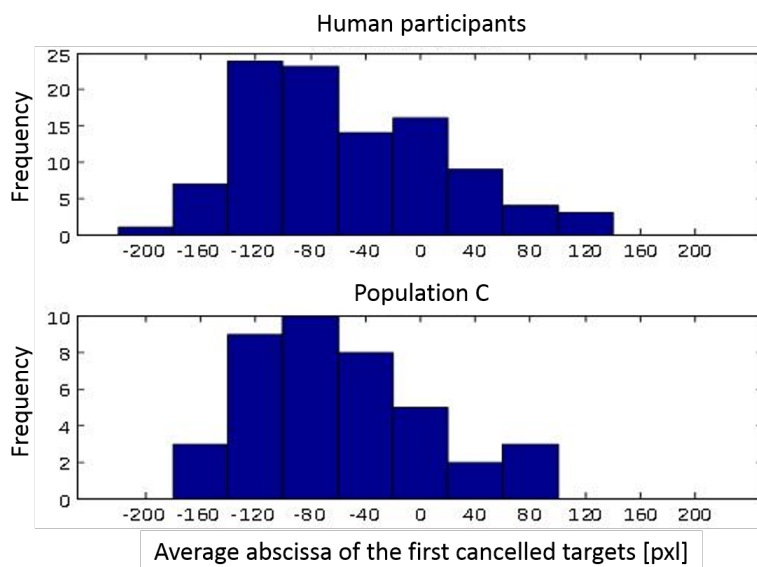


Figure 8. Distribution of the position of the first cancelled target for 101 human participants (see Experiment 1) and for the population of neurorobots equipped with the biologically inspired neurocontroller C.

4. General Discussion

In this study, we established specific connectivity constraints leading to a lateral spatial bias (pseudoneglect) in artificial organisms trained to perform a visual search task by using genetic algorithms. A form of pseudoneglect that was qualitatively and quantitatively similar to that shown by normal participants did emerge in artificial neurorobots, but only in those harboring hemispheric asymmetries of connectivity that simulated those typically occurring in the human brain. As a further condition, a general excitatory influence of VAN on the ipsilateral DAN was necessary for pseudoneglect to occur in neurorobots. This novel result suggests that hemispheric asymmetry alone is not sufficient to generate a leftward bias, and thus further specifies the likely connectional constraints of pseudoneglect.

In their recent review, Borji and Itti [42] provided a taxonomy of nearly 65 computational models of visual attention. Many of these models focused on reproducing eye movements (e.g., the saliency-based models reported in Borji and Itti [42]), following a bottom up approach. Typically, these models extract a set of features, represented as maps, from an incoming image. Then, feature maps are combined in a saliency map where a winner-take-all mechanism will designate the spatial region to be attended. Saliency-based attention models in general do not account for exploration biases, with the exception of a recent model [43], where an object center bias (the tendency to focus on the center of objects) is reproduced by adding an ad-hoc bias map to the saliency map. While important for building predictive models, this result seems little relevant to lateral biases such as pseudoneglect. Other models [44, 45] simulate attention as emerging from the competition of several brain areas subjected to bottom-up and top-down biases. These models do not drive eye movements; the scan path is simulated as a sequence of activations of the simulated posterior parietal cortex. Lanyon and Denham [46, 47] added to these models simulated eye movements and an

adjustable attention window scaled according to stimuli density. Despite being successful at reproducing scan paths in healthy individuals and neglect patients, these models do not address the issue of pseudoneglect. Other models of attention did not consider pseudoneglect because of their training procedure or design constraints [41, 48-50]. Di Ferdinando et al. [51] explored line bisection and target cancellation performance in four biologically inspired neural networks. The networks' patterns of connectivity varied along different degrees of asymmetry, inspired by specific theories. Pseudoneglect occurred in line bisection but not in visual search. In these models, motor outputs were only used for target selection; there was no active exploration of the environment, whereas when our neurorobots explored their environment the corresponding input information changed as a function of eye movements. Nonetheless, the present study shares with Di Ferdinando et al. [51] and other work from the Zorzi group [52] the stress on accounts of attentional phenomena relying on sensory-motor transformations, as stated by the premotor theory of attention [53].

Thus, at variance with most available models of attention, our artificial robots are trained to correctly cancel target stimuli, and are free to self-organize in order to find a proper solution, within the sole limits of the imposed connectivity constraints. These constraints were inspired by available data concerning the anatomical and functional organization of the attentional networks in the human brain [24, 25, 34]. To the best of our knowledge, this is the first attempt to simulate the dorsal and ventral attention networks in the two hemispheres of the human brain. Another original feature of the present models is the embodiment factor, consisting of the explicit modeling of eye and hand movements (see also Refs. [41, 46, 54-56]). In particular, the present models extended the models devised by Di Ferdinando et al [41], by increasing the complexity of the organisms' retina, the biological plausibility of the motor system and that of the neural controllers. Conti et al. [57] also adopted an embodied perspective, based on a humanoid robot

platform. In their study, an iCub robot was trained to remove objects from a table, a task reminiscent of a cancellation task. Intra-hemispheric disconnections were able to produce neglect-like behavior. However, the embodiment of the model was limited by the facts that selection of a visual target was carried out independently of the motor behavior, and that robot's eyes were kept fixed during the cancellation task. Moreover, although hemisphere asymmetry was modeled by increasing the number of right hemisphere processing units, no bias in normal performance is reported.

Moreover, at variance with most published work, our model attempted to simulate the relationships between the visual pathways and the attentional networks by respecting important biological constraints. Visual pathways project mainly to the hemisphere contralateral to each visual field. However, theoretical models of visual attention posit that the left hemisphere mainly deals with the contralateral hemispace, whereas the right hemisphere has a more bilateral competence [22, 58]. In previous computational models this asymmetry has not always been simulated in a biologically plausible way. In some cases, both simulated hemispheres received visual information from the whole visual field, with attention asymmetries being represented in inner layers [41, 49]. In the Conti et al.'s model [57], the right hemisphere received information from both visual hemifields, whereas the left hemisphere processes only the contralateral visual hemifield. However, there is no anatomical evidence of such asymmetries in the visual pathways, and information exchange in the occipital visual areas is mainly limited to the vertical meridian [59]. In our model, these important biological constraints of visual information processing were respected, because each artificial hemisphere received visual information from the contralateral hemifield; inter-hemispheric connections were only present at a later stage of processing, between the artificial DANs.

Finally, we note that the present population-based model can be potentially used to explore in a natural manner the universal properties (the basic brain architecture) and individual differences in network efficiency, two aspects recently underlined by Michael Posner [60] as appropriate features for future models of attention.

In conclusion, we have demonstrated the emergence of pseudoneglect behavior in artificially evolving neurorobots searching for visual objects, under specific connectional constraints. These neurorobots provide a plausible model for the dynamic interactions between fronto-parietal attention networks in the human brain.

5. References

1. Bowers D, Heilman KM. Pseudoneglect: Effects of hemispace on a tactile line bisection task. *Neuropsychologia*. 1980;18:491-8.
2. Jewell G, McCourt ME. Pseudoneglect: a review and meta-analysis of performance factors in line bisection tasks. *Neuropsychologia*. 2000;38(1):93-110. Epub 2000/01/05. doi: S0028-3932(99)00045-7 [pii]. PubMed PMID: 10617294.
3. Urbanski M, Bartolomeo P. Line bisection in left neglect: The importance of starting right. *Cortex*. 2008;44(7):782-93.
4. Bartolomeo P, D'Erme P, Gainotti G. The relationship between visuospatial and representational neglect. *Neurology*. 1994;44:1710-4.
5. Azouvi P, Bartolomeo P, Beis J-M, Perennou D, Pradat-Diehl P, Rousseaux M. A battery of tests for the quantitative assessment of unilateral neglect. *Restorative Neurology and Neuroscience*. 2006;24(4-6):273-85.
6. Brooks JL, Sala SD, Logie RH. Tactile rod bisection in the absence of visuo-spatial processing in children, mid-age and older adults. *Neuropsychologia*. 2011;49(12):3392-8. doi: <http://dx.doi.org/10.1016/j.neuropsychologia.2011.08.015>.
7. Ossandón JP, Onat S, König P. Spatial biases in viewing behavior. *Journal of Vision*. 2014;14(2):20. doi: 10.1167/14.2.20. PubMed PMID: 24569986.
8. Foulsham T, Gray A, Nasiopoulos E, Kingstone A. Leftward biases in picture scanning and line bisection: A gaze-contingent window study. *Vision Research*. 2013;78:14-25. doi: <http://dx.doi.org/10.1016/j.visres.2012.12.001>.
9. Benedetto S, Pedrotti M, Bremond R, Baccino T. Leftward attentional bias in a simulated driving task. *Transportation Research Part F: Traffic Psychology and Behaviour*. 2013;20:147-53. doi: <http://dx.doi.org/10.1016/j.trf.2013.07.006>.
10. Nicholls MER, Loftus AM, Orr CA, Barre N. Rightward collisions and their association with pseudoneglect. *Brain and Cognition*. 2008;68(2):166-70. doi: <http://dx.doi.org/10.1016/j.bandc.2008.04.003>.
11. Hatin B, Sykes Tottenham L, Oriet C. The relationship between collisions and pseudoneglect: Is it right? *Cortex*. 2012;48(8):997-1008. doi: <http://dx.doi.org/10.1016/j.cortex.2011.05.015>.
12. Śmigasiewicz K, Westphal N, Verleger R. Leftward bias in orienting to and disengaging attention from salient task-irrelevant events in rapid serial visual presentation. *Neuropsychologia*. 2017;94:96-105. doi: <http://dx.doi.org/10.1016/j.neuropsychologia.2016.11.025>.
13. Coolican J, Eskes GA, McMullen PA, Lecky E. Perceptual biases in processing facial identity and emotion. *Brain and Cognition*. 2008;66(2):176-87. doi: <http://dx.doi.org/10.1016/j.bandc.2007.07.001>.
14. Brooks J, Della Sala S, Darling S. Representational Pseudoneglect: A Review. *Neuropsychol Rev*. 2014;24(2):148-65. doi: 10.1007/s11065-013-9245-2.
15. Burlon C, Oliviero B, Wattiez N, Pouget P, Bartolomeo P. Visual mental imagery: What the head's eye tells the mind's eye. *Brain Res*. 2011;1367:287-97.
16. Azouvi P, Samuel C, Louis-Dreyfus A, Bernati T, Bartolomeo P, Beis J-M, et al. Sensitivity of clinical and behavioural tests of spatial neglect after right hemisphere stroke. *J Neurol Neurosurg Psychiatr*. 2002;73(2):160-6.
17. Gainotti G, D'Erme P, Bartolomeo P. Early orientation of attention toward the half space ipsilateral to the lesion in patients with unilateral brain damage. *J Neurol Neurosurg Psychiatr*. 1991;54:1082-9.
18. McCourt ME, Garlinghouse M, Reuter-Lorenz PA. Unilateral visual cueing and asymmetric line geometry share a common attentional origin in the modulation of pseudoneglect. *Cortex*. 2005;41(4):499-511. Epub 2005/07/27. PubMed PMID: 16042026.
19. Toba MN, Cavanagh P, Bartolomeo P. Attention biases the perceived midpoint of horizontal lines. *Neuropsychologia*. 2011;49(2):238-346.

20. Chokron S, Imbert M. Influence of reading habits on line bisection. *Cognitive Brain Research*. 1993;1:219-22.
21. McCourt ME, Jewell G. Visuospatial attention in line bisection: stimulus modulation of pseudoneglect. *Neuropsychologia*. 1999;37(7):843-55. Epub 1999/07/17. doi: S0028-3932(98)00140-7 [pii]. PubMed PMID: 10408651.
22. Heilman KM, Van Den Abell T. Right hemisphere dominance for attention: the mechanism underlying hemispheric asymmetries of inattention (neglect). *Neurology*. 1980;30(3):327-30.
23. Mesulam M-M. Spatial attention and neglect: parietal, frontal and cingulate contributions to the mental representation and attentional targeting of salient extrapersonal events. *Philosophical Transactions of the Royal Society of London B*. 1999;354(1387):1325-46. PubMed PMID: 10466154.
24. Thiebaut de Schotten M, Dell'Acqua F, Forkel SJ, Simmons A, Vergani F, Murphy DGM, et al. A lateralized brain network for visuospatial attention. *Nature Neuroscience*. 2011;14(10):1245-6. doi: 10.1038/nn.2905.
25. Corbetta M, Shulman GL. Control of goal-directed and stimulus-driven attention in the brain. *Nat Rev Neurosci*. 2002;3(3):201-15.
26. Corbetta M, Shulman GL. Spatial neglect and attention networks. *Annu Rev Neurosci*. 2011;34:569-99. Epub 2011/06/23. doi: 10.1146/annurev-neuro-061010-113731. PubMed PMID: 21692662.
27. Bartolomeo P, Thiebaut de Schotten M, Chica AB. Brain networks of visuospatial attention and their disruption in visual neglect. *Front Hum Neurosci*. 2012;6:110. doi: doi: 10.3389/fnhum.2012.00110.
28. Posner MI. Orienting of attention. *The Quarterly Journal of Experimental Psychology*. 1980;32:3-25.
29. Nobre AC, Sebestyen GN, Gitelman DR, Mesulam MM, Frackowiak RS, Frith CD. Functional localization of the system for visuospatial attention using positron emission tomography. *Brain*. 1997;120:515-33.
30. Bourgeois A, Chica AB, Valero-Cabré A, Bartolomeo P. Cortical control of inhibition of return: causal evidence for task-dependent modulations by dorsal and ventral parietal regions. *Cortex*. 2013;49(8):2229-38. doi: 10.1016/j.cortex.2012.10.017. PubMed PMID: 23332817.
31. Bourgeois A, Chica AB, Valero-Cabré A, Bartolomeo P. Cortical control of Inhibition of Return: exploring the causal contributions of the left parietal cortex. *Cortex*. 2013;49(10):2927-34. doi: 10.1016/j.cortex.2013.08.004. PubMed PMID: 24050220.
32. Salazar R, Dotson N, Bressler S, Gray C. Content-specific fronto-parietal synchronization during visual working memory. *Science*. 2012;338(6110):1097-100.
33. Marzi CA. Asymmetry of interhemispheric communication. *Wiley Interdisciplinary Reviews: Cognitive Science*. 2010;1(3):433-8. doi: 10.1002/wcs.53. PubMed PMID: 9404205376883890958related:Dpv78_ZygoJJ.
34. Koch G, Cercignani M, Bonni S, Giacobbe V, Bucchi G, Versace V, et al. Asymmetry of parietal interhemispheric connections in humans. *J Neurosci*. 2011;31(24):8967-75. doi: 10.1523/jneurosci.6567-10.2011. PubMed PMID: 21677180; PubMed Central PMCID: PMC21677180.
35. Catani M, Thiebaut de Schotten M. *Atlas of the Human Brain Connections*: Oxford University Press; 2012.
36. Patel GH, Yang D, Jamerson EC, Snyder LH, Corbetta M, Ferrera VP. Functional evolution of new and expanded attention networks in humans. *Proc Natl Acad Sci U S A*. 2015;112(30):9454-9. doi: 10.1073/pnas.1420395112. PubMed PMID: 26170314; PubMed Central PMCID: PMC4522817.
37. Rousseaux M, Beis JM, Pradat-Diehl P, Martin Y, Bartolomeo P, Chokron S, et al. Normalisation d'une batterie de dépistage de la négligence spatiale. Etude de l'effet de l'âge, du niveau d'éducation, du sexe, de la main et de la latéralité [Presenting a battery for assessing spatial neglect. Norms and effects of age, educational level, sex, hand and laterality]. *Revue Neurologique*. 2001;157:1385-401.

38. Eriksen CW, Yeh Y-Y. Allocation of attention in the visual field. *Journal of Experimental Psychology: Human Perception and Performance*. 1985;11(5):583-97.
39. Massera G, Ferrauto T, Gigliotta O, Nolfi S. Designing adaptive humanoid robots through the FARSA open-source framework. *Adaptive Behavior*. 2014;1059712314536909.
40. Nolfi S, Floreano D. *Evolutionary Robotics: The Biology, Intelligence, and Technology*: MIT Press; 2000. 320 p.
41. Di Ferdinando A, Parisi D, Bartolomeo P. Modeling orienting behavior and its disorders with "ecological" neural networks. *Journal of Cognitive Neuroscience*. 2007;19(6):1033-49.
42. Borji A, Itti L. State-of-the-Art in Visual Attention Modeling. *IEEE Transactions on Pattern Analysis and Machine Intelligence*. 2013;35(1):185-207. doi: 10.1109/TPAMI.2012.89.
43. Borji A, Tanner J. Reconciling saliency and object center-bias hypotheses in explaining free-viewing fixations. *IEEE transactions on neural networks and learning systems*. 2016;27(6):1214-26.
44. Deco G, Rolls ET. A neurodynamical cortical model of visual attention and invariant object recognition. *Vision research*. 2004;44(6):621-42.
45. Deco G, Zihl J. A biased competition based neurodynamical model of visual neglect. *Medical Engineering & Physics*. 2004;26(9):733-43. doi: <http://dx.doi.org/10.1016/j.medengphy.2004.06.011>.
46. Lanyon LJ, Denham SL. A model of active visual search with object-based attention guiding scan paths. *Neural Networks*. 2004;17(5):873-97.
47. Lanyon LJ, Denham SL. Modelling visual neglect: computational insights into conscious perception. *PLoS One*. 2010;5(6):e11128.
48. Mozer MC. Frames of reference in unilateral neglect and visual perception: a computational perspective. *Psychological Review*. 2002;109(1):156-85.
49. Monaghan P, Shillcock R. Hemispheric asymmetries in cognitive modeling: connectionist modeling of unilateral visual neglect. *Psychological Review*. 2004;111(2):283-308. PubMed PMID: 15065911.
50. Pouget A, Sejnowski TJ. Simulating a lesion in a basis function model of spatial representations: comparison with hemineglect. *Psychological Review*. 2001;108(3):653-73.
51. Di Ferdinando A, Casarotti M, Vallar G, Zorzi M. Hemispheric asymmetries in the neglect syndrome: a computational study. In: Cangelosi A, Bugmann G, Borisyuk R, editors. *Modelling Language, Cognition and Action*. Singapore: World Scientific; 2005. p. 249-58.
52. Casarotti M, Lisi M, Umiltà C, Zorzi M. Paying attention through eye movements: a computational investigation of the premotor theory of spatial attention. *J Cogn Neurosci*. 2012;24(7):1519-31. Epub 2012/03/29. doi: 10.1162/jocn_a_00231. PubMed PMID: 22452561.
53. Rizzolatti G, Riggio L, Dascola I, Umiltà C. Reorienting attention across the horizontal and vertical meridians: evidence in favor of a premotor theory of attention. *Neuropsychologia*. 1987;25(1A):31-40. Epub 1987/01/01. PubMed PMID: 3574648.
54. Gigliotta O, Bartolomeo P, Miglino O. *Introducing Sensory-motor Apparatus in Neuropsychological Modelization*. Connection Science. 2014.
55. Miglino O, Ponticorvo M, Bartolomeo P. Place cognition and active perception: a study with evolved robots. *Connection Science*. 2009;21(1):3-14.
56. Bartolomeo P, Pagliarini L, Parisi D. Emergence of orienting behavior in ecological neural networks. *Neural Processing Letters*. 2002;15(1):69-76.
57. Conti D, Di Nuovo S, Cangelosi A, Di Nuovo A. Lateral specialization in unilateral spatial neglect: a cognitive robotics model. *Cognitive processing*. 1-8.
58. Mesulam MM. A cortical network for directed attention and unilateral neglect. *Annals of Neurology*. 1981;10:309-25.

59. Berlucchi G. Visual interhemispheric communication and callosal connections of the occipital lobes. *Cortex*. 2014;56:1-13.
60. Posner MI. Guides to the study of attention. In: Nobre AC, Kastner S, editors. *The Oxford Handbook of Attention*. Oxford: Oxford University Press; 2014. p. 1-5.